ELECTRO-OPTICAL PROPERTIES OF SINGLE-WALL MOLYBDENUM-DISULPHIDE NANOTUBES

Božidar Nikolić, Ivanka Milošević and Milan Damnjanović
Nanostructure Laboratory, Faculty of Physics, POB 368, Belgrade 11001, Serbia

Invited Paper

Abstract – *Electro-optical properties of MoS_2 nanotubes are considered. To this end the necessity of the relaxation of the simply folded layer configuration is analyzed, and three regions are found: when it is necessary (narrow tubes), when it can be simulated by the layer stretching (tubes of diameters within 50-200Å), and when it can be avoided (thick tubes). Full symmetry implemented density-functional tight-binding method is used to find the electronic bands for number of tubes of different chirality, and some characteristics (direct/indirect gap chirality and diameter dependence) of the band structures are singled out. Finally, optical transitions selection rules are derived and used to calculate optical response functions.*

1 INTRODUCTION

Although the transition metal disulfide nanotubes have been synthesized [1, 2] soon after the discovery of the carbon ones, their theoretical studies are restricted to very few papers on electronic band calculations [3, 4], symmetry [5] and Raman active phonon modes [6]. On the other hand, there is a number of experimental reports on optical absorption [7], Raman spectra [8], field emission [9] and shear and Young's moduli [10] measurements. Here we start analysis of the optical spectra of MoS2 nanotubes.

2 FOLDED CONFIGURATION AND SYMMETRY

Symmetry and the classification of single wall MoS_2 nanotubes is determined with the help of the symmetry of an unfolded diperiodic layer, in the same way as for carbon nanotubes.

Single MoS_2 layer (Fig. 1) consists of two parallel hexagonal sulfur planes at the distance $2\delta = 6.37\,\text{Å}$, with lattice vectors $\mathbf{a}_1$ and $\mathbf{a}_2$ of the length $a_0 = 3.16\,\text{Å}$. Configuration with sulfur atoms of different planes one just above another is preferable. Molybdenum plane, in the middle of the sulphur ones, has the same lattice, only the atoms (dark circles) are translated by $(\mathbf{a}_1 + \mathbf{a}_2)/3$, being thus at the centres of the sulphur triangles. This way, elementary cell contains two sulfur and one molybdenum atoms. The single layer symmetry group is diperiodic group **Dg78** ($p\tilde{6}m2$).

Single-wall MoS_2 nanotube (n_1, n_2) can be viewed as the layer folded such that the *chiral vector* $\mathbf{c} = n_1\mathbf{a}_1 + n_2\mathbf{a}_2$ becomes circumferential of the cylinder. Obviously, the pair (n_1, n_2) uniquely determines all the structural properties of the corresponding nanotubes. Particularly, the symmetry of the nanotube is described by one of the line groups [5]: chiral (n_1, n_2), zig-zag, $(n, 0)$, and armchair

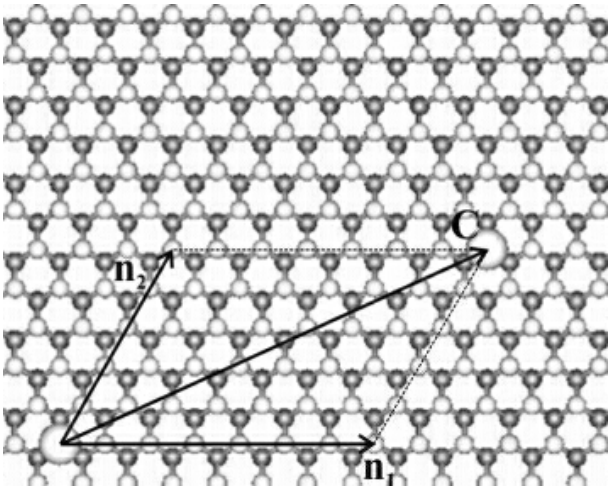

Figure 1: *MoS_2 single layer. Open circles stand for the sulfur, and filled ones for the molybdenum atoms.*

tubes (n, n) (shown in Fig. 2) have line groups from the first, eighth and fourth family, respectively:

$$\begin{aligned} \mathbf{L}_{\mathcal{C}} &= \mathbf{T}^r_q(a)\mathbf{C}_n, \\ \mathbf{L}_{\mathcal{Z}} &= \mathbf{T}^1_{2n}(a_0\sqrt{3})\mathbf{C}_{nv}, \\ \mathbf{L}_{\mathcal{A}} &= \mathbf{T}^1_{2n}(a_0)\mathbf{C}_{nh}. \end{aligned} \tag{1}$$

Here, $\mathbf{T}^r_q(a)$ is screw-axis generated by the transformation $(C^r_q|an/q)$ (Koster-Seitz symbol), while the remaining factors $\mathbf{C}_n$, $\mathbf{C}_{nv}$ and $\mathbf{C}_{nh}$ are point groups. The orders of the rotational axis of the point factor (n) and isogonal group (q), translational period (a) and helicity parameter (r) are:

$$n = \text{GCD}(n_1, n_2), \tag{2}$$

$$a = \frac{\sqrt{3(n_1^2 + n_2^2 + n_1 n_2)}}{n\mathcal{R}} a_0 \tag{3}$$

$$q = 2\frac{n_1^2 + n_1 n_2 + n_2^2}{n\mathcal{R}}, \tag{4}$$

$$r = \frac{n_1 + 2n_2 - (\frac{n_2}{n})^{\phi(\frac{n_1}{n})-1} q\mathcal{R}}{n_1\mathcal{R}} \pmod{\frac{q}{n}}, \tag{5}$$

($\mathcal{R} = \text{GCD}(2n_1 + n_2, n_1 + 2n_2)/n$, ϕ is Euler's function).

Single wall tubes are three-orbit systems, i.e. their *symmcell* (the set of orbit representatives, i.e. the minimal set of atoms from which the symmetry group generates the whole structure) contains two sulfur and one molybdenum atom (Fig. 2, upper left panel). Positions of these representative atoms are also defined by the tube indices n_1 and n_2:

$$S_{\text{in}}: \qquad \left(\frac{D-\delta}{2}, 0, 0)\right),$$

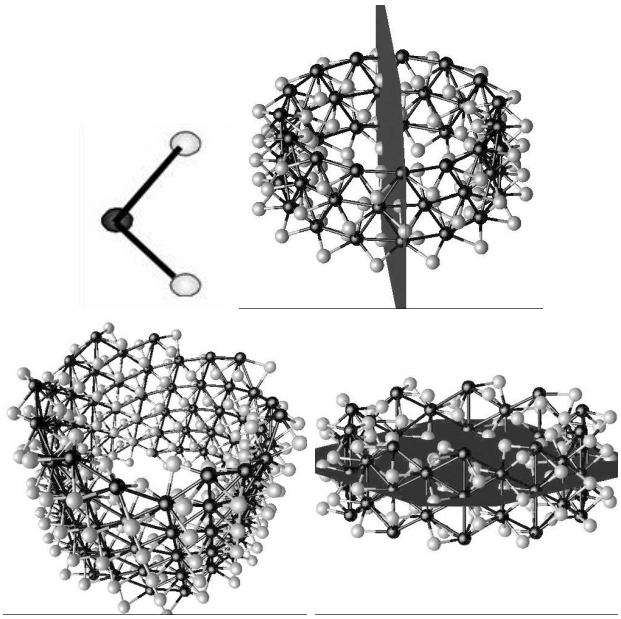

Figure 2: *Symmcell and tubes of different types (zig-zag (15,0), chiral (13,7) and armchair (10,10)).*

$$S_{\text{out}}: \quad \left(\frac{D+\delta}{2}, 0, 0\right), \tag{6}$$
$$Mo: \quad \left(\frac{D}{2}, \varphi_0, z_0\right),$$

where the molybdenum layer diameter is

$$D = a_0\sqrt{n_1^2 + n_1 n_2 + n_2^2}, \tag{7}$$

while, the φ and z cylindrical coordinates of the molybdenum symcell atom (x-axis is chosen through the sulfur atoms) are:

$$\varphi_0 = \pi\frac{n_1 + n_2}{n_1^2 + n_1 n_2 + n_2^2}, \tag{8}$$
$$z_0 = \frac{a_0}{2\sqrt{3}}\frac{n_1 - n_2}{\sqrt{n_1^2 + n_1 n_2 + n_2^2}}. \tag{9}$$

3 RELAXATION

However, the described rolled-up layer configuration is not equilibrium one, as the curvature induced additional tensions with respect to layer. Therefore density functional relaxation method is applied to find the stable configuration. The symmetry is implemented also in these calculations. In fact, instead of varying all the atomic coordinates, we apply the topological theorem [11] that the extremes of the invariant functions are on the manifolds with extremal symmetry. Therefore, only the coordinates along which the symmetry is not decreasing (with respect to simply folded configuration) are varied. Obviously, this means that only symcell atoms coordinates are degrees of freedom. Precisely, choosing x axis through the interior sulfur atom, it remains to check only its diameter, and six coordinates of molybdenum and outer sulphur. For zig-zag tubes, to preserve vertical mirror plane also φ of the last two atoms is fixed to zero, as well as in the armchair tubes, due to the horizontal mirror plane z coordinates vanishes. In addition, the translational period of the tube is varied, as the only continual symmetry parameter.

We performed density functional relaxation within tight-binding [12] prescription (DFTB). It turns out that for the tubes with diameters greater than 200 Å the relaxation effects are negligible, while between 60 Å and 200 Å relaxed configuration is very well described as the rolled-up one, but with the layer with the increased lattice constant a_0 for 0.25 Å. Below 60 Å, various effects of curvature can be seen.

As the usually synthesized tubes have diameters greater than 200 Å, they can be treated without relaxation. However, most of their properties are similar to the bulk. Therefore, the most interesting tubes are with the diameters less than 50 Å, and for them the relaxation procedure is necessary, but it can be substituted by the stretching of the layer. Finally, for the narrow tubes the relaxation is unavoidable.

4 ELECTRONIC BANDS

Electronic bands are calculated numerically, implementing the full line group symmetry. Underlying theoretical methods are based on the modified Wigner projectors technique (MGPT) [13]. In solid state physics, Bloch theorem enables to reduce the eigenproblem to the elementary cell; however, in the case of nanotubes elementary cell contains huge number of atoms, and usual methods of diagonalization of hamiltonian are time consuming, or even non applicable on available computers. Recently, the method has been developed to reduce exactly the eigenproblems to symcell. Also, instead of the whole symmetry group, only the generators are used. This technique is fully implemented within POLSym code [14], designed for symmetry based calculations of electronic, phonon and photonic bands, their assignation by the complete set of the conserved quantum numbers, and various applications.

Electronic bands and the corresponding generalized Bloch functions are calculated within tight binding approximation, using the density functional input data for (radius vector dependent) two-center hamiltonian and overlap matrix elements. The atomic orbitals are the Slater type ones, obtained also by the density functional method [12, 3]. Particularly, for the sulphur atom one $3s$ and three $3p$ Slater type orbitals are used, while one $5s$, three $5p$ and five $4d$ orbitals for molybdenum. The electronic bands are calculated for a number of nanotubes.

Results for the tubes (35,35) and (60,0) are shown in Fig. 3 and Fig. 4. In general, according to the symmetry, the bands, together with the corresponding Bloch eigenfunctions are assigned by the angular momentum quantum number m. Only for the achiral tubes there is also a parity quantum number: for zig-zag tubes, vertical mirror parity $\Pi^v = \pm 1$ characterizes $m = 0$ and $m = n$ bands throughout Brillouin zone, while for armchair ones, $\Pi^h = \pm 1$ is relevant for the same bands but only in the Γ point.

Some significant conclusions can be made directly from the electronic bands structures. The tubes are semiconducting, with the gap slightly increasing with the diameter, and rapidly saturating at the value of 1.5 eV of MoS_2

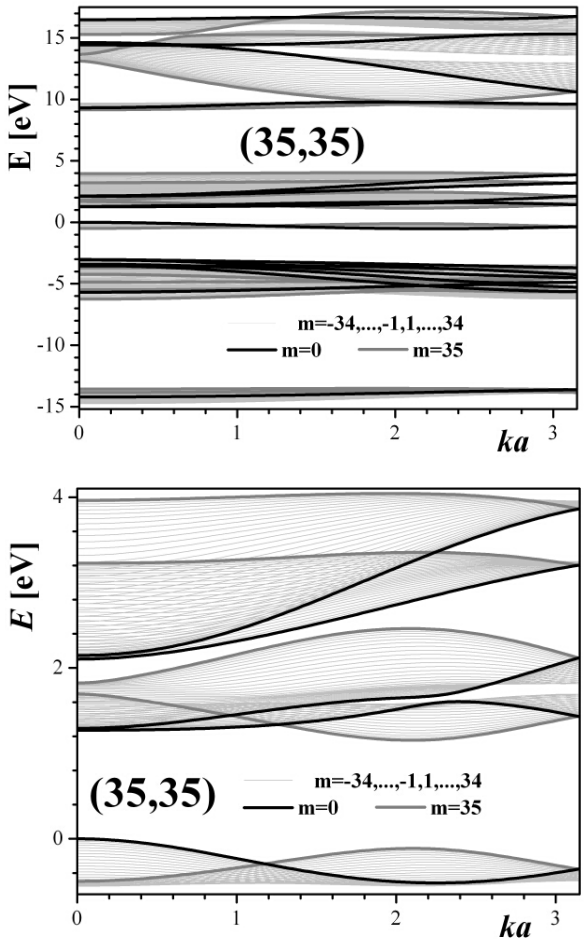

Figure 3: *Electronic bands of the armchair tube (35,35). Upper panel: whole DFTB band structure. Lower panel: vicinity of the Fermi level.*

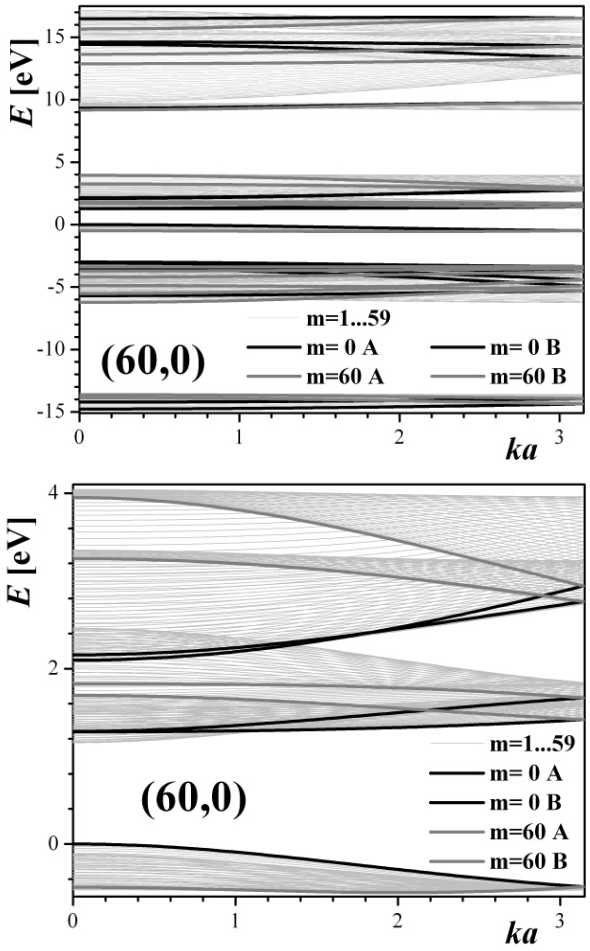

Figure 4: *Electronic bands of zig-zag tube (60,0). Upper panel: whole DFTB band structure. Lower panel: vicinity of the Fermi level.*

bulk ($D = \infty$ limit). Near Fermi level structure of the same diameter tubes is chirality dependent. This is illustrated in the Fig. 3 and Fig. 4, for the same diameter $D \sim 60\,\text{Å}$ nanotubes (60,0) and (35,35). The gap of the both tubes is about 1.2 eV. However, the former one is direct gap semiconductor with the highest occupied molecular orbital (HOMO) and lowest unoccupied molecular orbital (LUMO) at $k = 0$, while the armchair tube has indirect gap (HOMO at the center of the zone and LUMO at $k = \frac{2\pi}{3a}$). Still, the density of electronic states near Fermi level shows no significant difference (Fig. 5).

5 OPTICAL CONDUCTIVITY

All the optical response functions are derived from the optical conductivity tensor σ, which is within time dependent perturbation theory calculated from the band structure and corresponding Bloch eigenstates according to the expression:

$$\text{Re}[\sigma_{ab}(\omega)] = \frac{C}{\omega}\sum_{if}\langle i\,|\,p_a\,|\,f\rangle\langle f\,|\,p_b\,|\,i\rangle\delta(E_f - E_i - \hbar\omega)n_i(1-n_f). \tag{10}$$

Here E_f and E_i refer to the energies of the initial and final Bloch states $|i\rangle$ and $|f\rangle$. Therefore, it is important to find the transition matrix elements involved in 10. At first we employ the optical transitions selection rules

$$k_f = k_i, \quad m_f = m_i + m, \tag{11}$$

$$\Pi_f^v\Pi^v\Pi_i^v \neq -1 \quad \Pi_f^h\Pi^h\Pi_i^h \neq -1. \tag{12}$$

The last selection rules refer to the achiral tubes only. The calculations are performed for symmetry momentum components $p_0 = p_z$ and $p_\pm = p_x \mp \mathrm{i}p_y$, corresponding to the light polarized along tube axis (z), and perpendicular to it positive and negative circular polarization. For p_0 the quantum numbers are $k = 0$, $m = 0$, $\Pi_v = 1$ and $\Pi_h = -1$, while for $p_\pm$ one has $k = 0$, $m = \pm 1$, $\Pi_v = 0$ and $\Pi_h = 1$.

Direct consequence of symmetry is that the optical conductivity tensor σ of single wall MoS_2 tubes is diagonal with two independent tensor components [5]: $\sigma_{||} = \sigma_z = \sigma_{zz}$ and $\sigma_\perp = \sigma_{xx} = \sigma_{yy}$. Therefore only these two components are calculated.

Optical conductivity for narrow zig-zag tubes with diameters within 10-16 Å is shown on Figure 6. Optical conductivity for light polarized parallel to tube axis and for the perpendicular circular polarization is slightly dependent on tube diameter. Transition energies (position of

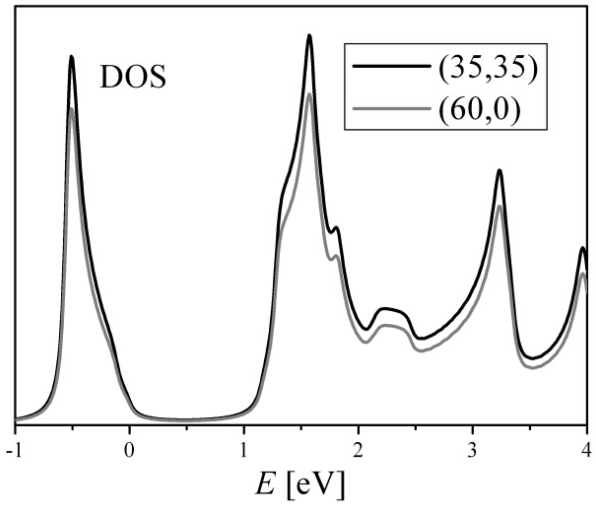

Figure 5: *Electron density of states for thick tubes.*

peaks) follow gap increase with the diameter. Note that the gap of these tubes is lower than 1 eV, being much less than in bulk or layered structure. In comparison with electro-optical properties of carbon nanotubes [15] some important differences are found. Absorption intensities for parallel and perpendicular polarization differs a lot, but intensity for parallel polarization is three or four times larger than intensity for perpendicular polarization. Absorption for parallel polarization in the case of carbon nanotubes is at least order of magnitude larger than absorption intensity for perpendicular polarization. Next difference is that the transition energies for parallel and perpendicular polarization are almost the same. In other words liner dichroism effect is weak. This effect is easy to understand in the view of huge number of bands near gap (Fig. 3 and Fig. 4), making always possible to find two close bands allowing transitions with both light polarizations.

For wider armchair tubes with D within 26-32 Å, the diameter signature in absorption spectrum vanishes (Fig. 7). In fact, the saturation is mostly achieved for this thickness, as visible also from the band gap: it is close to 1.5 eV, corresponding to bulk. Absorption intensity ratio remains close to narrow tubes, and dichroism is very weak, again.

Optical conductivity for three wide tubes with almost the same diameter and different chirality is shown in Figure 8. Absorption energies are the same for all tubes but intensities are different. Armchair tube absorbs light for any polarization more intense than zig-zag and chiral tube. The vanishing of diameter dependence in absorption spectrum of wide tubes shows that DFTB based calculation has a good limit, or absorption spectrum becomes close to bulk one as diameter increasing.

6 SUMMARY

The full symmetry implemented electronic band calculation of MoS_2 nanotubes is used to predict some of the optical properties of these structures. It is observed that the diameter dependence of the gap is clearly manifested in the optical spectra, which can be applied in the optical

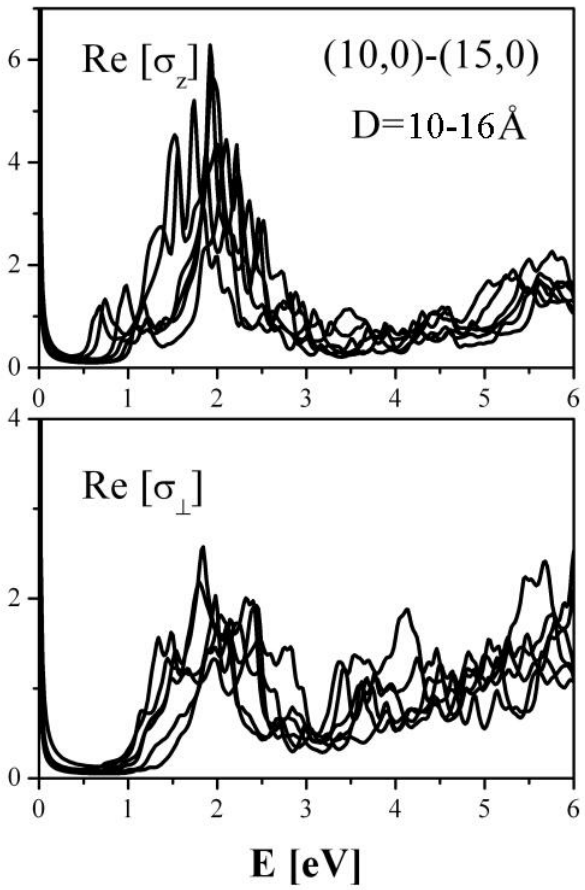

Figure 6: *Optical conductivity for zig-zag tubes.*

nanodevices. However, this effect saturates for the tube thickness larger than 30 Å. The chirality of the tubes determine if the gap is direct or not. Also, it is stressed out that for the synthesized tubes the configuration is either purely folded one (for thick tubes) or folded after layer stretching (tubes with diameters 60-200 Å).

Acknowledgements

This work was supported by Serbian Ministry of Science (project MNTR-1924), Slovenian-Serbian project BI-CS/04-05-037, and German DAAD projects A/0406460, A/0406461. Authors are grateful to Dr. Maja Remškar (Jozef Stefan Institute, Ljubljana) for samples, experimental data and fruitful discussion, and to Prof. Gotthard Seifert (TU Dresden) for DFTB calculated electron STO functions and hamiltonian/overlap matrix elements.

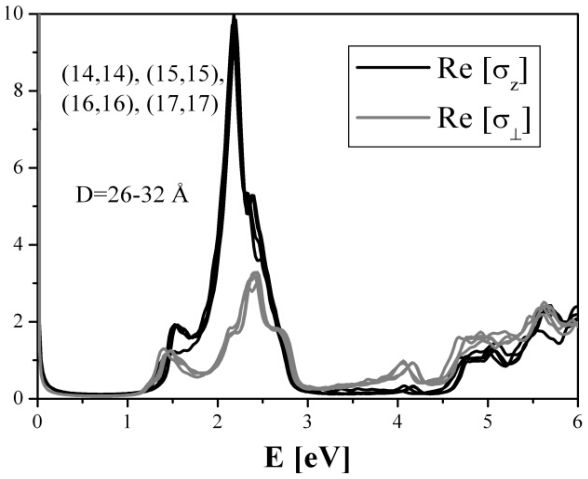

Figure 7: *Optical conductivity for armchair tubes.*

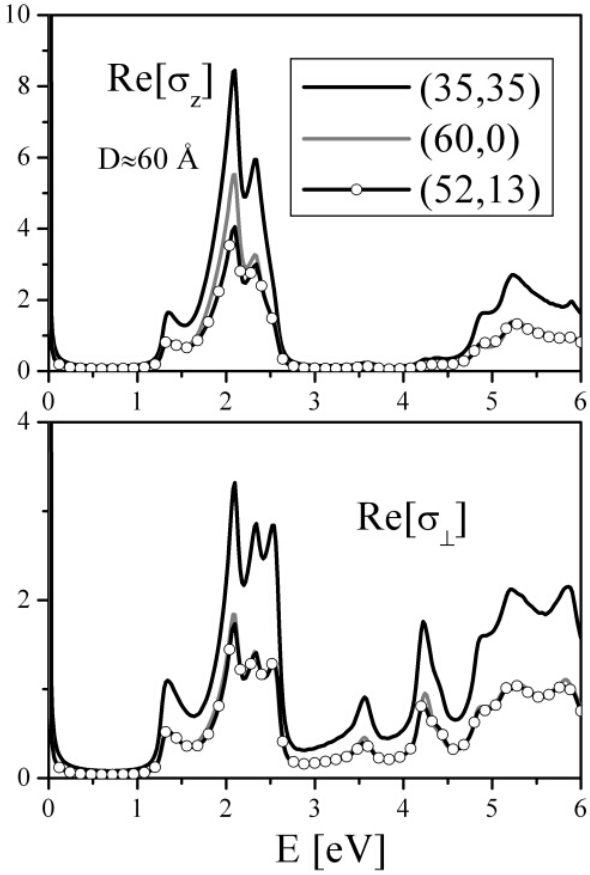

Figure 8: *Optical conductivity for thick tubes.*

References

[1] R. Tenne, M. Homyonfer and Y. Feldman, Chem. Mater. **10** (1998) 3225.

[2] M. Remškar, Adv. Matter. **16**, 1 (2004).

[3] G. Seifert, H. Terrones, M. Terrones, G. Jungnickel, and Thomas Frauenheim, Phys. Rev. Lett. **85**, (2000) 146. G. Seifert, T. Köhler, and R. Tenne, J. Phys. Chem. **106**, (2002) 2497.

[4] M. Verstraete and J.-C. Charlier, Phys. Rev. B **68** (2003) 045423.

[5] I. Milošević, T. Vuković, M. Damnjanović, and B. Nikolić, Eur. Phys. J. B **17** (2000) 707.

[6] E. Dobardžić, B. Dakić, M. Damnjanović and I. Milošević, Phys. Rev. B **71** (2005) 121405(R).

[7] G. L. Frey, S. Elani, M. Homyonfer, Y. Feldman and R. Tenne, Phys. Rev. B **57** (1998) 6666.

[8] G. L. Frey, R. Tenne, M. J. Matthews, M. S. Dresselhaus, and G. Dresselhaus, Phys. Rev. B **60**, (1999) 2883.

[9] V. Nemanič, M. Žumer, B. Zajec, J. Pahor, Maja Remškar, A. Mrzel, P. Panjan and D. Mihailović, Appl. Phys. Lett. **82** (2003) 4573.

[10] A. Kis, D. Mihailović, M. Remškar, A. Mrzel, A.Jesih, I. Piwinski, A. J. Kulik, W. Benoit, L. Forro, Adv. Matter. **15** (2003) 733.

[11] H. Abud and G. Sartori, Ann. Phys. **150** (1983) 307.

[12] D. Porezag, Th. Frauenheim, Th. Köhler, G. Seifert and R. Kaschner, *Phys. Rev. B* **51** 12947 (1995).

[13] M. Damnjanović, T. Vuković and I. Milošević, J. Phys. A **33** (2000) 6561.

[14] I. Milošević, A. Damjanović, and M. Damnjanović, in Quantum Mechanical Simulation Methods in Studying Biological Systems, edited by D. Bicout and M. Field (Springer-Verlag, Berlin, 1996) Chap. XIV.

[15] I. Milošević, T. Vuković, S. Dmitrović and M. Damnjanović, Phys. Rev. B **67** 165418 (2003).